Predictive Guidance Control for Autonomous Kites with Input Delay ⋆

Tony A. Wood * **Eva Ahbe** * **Henrik Hesse** ** **Roy S. Smith** *

* *Automatic Control Laboratory (IfA), ETH Zurich, Physikstrasse 3, 8092 Zurich, Switzerland.*
E-mail: {woodt, ahbee, rsmith}@control.ee.ethz.ch.
** *Aerospace Systems, University of Glasgow (Singapore), 510 Dover Road, Singapore 139660 (formerly at IfA, ETH Zurich).*
E-mail: henrik.hesse@glasgow.ac.uk.

Abstract: We consider the design of a model predictive guidance controller in a cascaded control scheme for an autonomous kite with significant input delay. The rate of change of the signal commanded by the guidance is bounded to ensure robust performance of the underlying tracking controller. We analyse the limitations of the tracking controller arising from model parameter uncertainty and input delay. The delay is accounted for in the control design by predicting the values of the feedback variables ahead of time based on the past inputs and the system models. To account for changing operating conditions the model parameters are updated online. The proposed method has been tested in a real-time hardware-in-the-loop simulation study.

Keywords: Airborne wind energy, renewable energy systems, predictive control, delay compensation, robust control, cascade control

1. INTRODUCTION

Airborne Wind Energy (AWE) generators extract wind power from aerodynamic forces acting on a tethered wing or kite. Such systems have been envisioned as an alternative to conventional wind turbines due to lower material costs and the ability of reaching higher altitudes where the wind is typically stronger and more consistent. To date, many different types of AWE systems exist and an overview of the field can be found in Ahrens et al. (2013).

We consider a ground-based kite system where power is generated at winches on the ground by unreeling tethers connected to a kite flying in crosswind motion, i.e. approximately perpendicular to the wind direction. The system operates in a periodic two-phase cycle as, for example, demonstrated in Zgraggen et al. (2015). In the so-called traction phase, power is generated by flying with high tether forces; in the retraction phase, the kite is reeled back in under low tether forces. In this work, we focus on the flight control during the traction phase. In particular, we consider the flight control of a two-line kite system with ground-based steering actuation. For experimental implementations of flight controllers, feedback variables relating to the kite flight direction have been shown to be useful in cascaded control approaches, see e.g. Erhard and Strauch (2013a); Fagiano et al. (2014). They employ model-free guidance strategies based on switching reference signals to fly figure-of-eight patterns.

⋆ This research was supported by the Swiss National Science Foundation (Synergia) No. 141836 and the European Union Horizon 2020 research and innovation programme under the Marie Sklodowska-Curie grant agreement No. 642682.

The steering control performance, especially for ground-based systems with line angle measurements, can be affected by estimation and actuation delay. Kite state estimation given output delay is addressed in Polzin et al. (2017). In Wood et al. (2015a) the estimated kite heading angle was related to the steering input with a model that includes an input delay. This model was applied to improve the tracking performance in the inner loop of the cascaded control approach in Fagiano et al. (2014).

Kinematic models have been proposed in Rontsis et al. (2015); Erhard and Strauch (2013b); Wood et al. (2015b) to further link the kite heading angle to the overall kite motion. In Rontsis et al. (2015) a kinematic model was used to develop a delay-compensating path controller which was experimentally demonstrated for constant line length. Wood et al. (2015b) also used a kinematic model including input delay to further improve the outer loop of the control approach in Fagiano et al. (2014). The proposed method includes a figure-of-eight path planning strategy in which limitations on the tracking bandwidth imposed by the input delay are considered. Online identification of the model parameters, the input delay and steering gain, allowed adaptation of the reference path to varying limitations during the traction phase, e.g. those arising from varying wind conditions and winch settings.

In this work, we extend the guidance strategy in Wood et al. (2015b) by formulating an optimisation problem with constraints on the input, input rate, and on the kite position. Respecting the input rate constraint in the cascaded control architecture ensures robust tracking performance of the underlying controller. Model Predictive Control (MPC) is an optimisation based method that accounts for constraints on the states and inputs of a

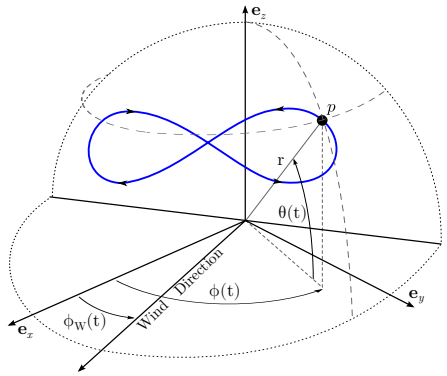

Fig. 1. Kite position, p, in the ground coordinate frame, (e_x, e_y, e_z), related to the elevation angle, θ, azimuth angle, ϕ, and wind window for line length, r.

control system. MPC applied to kites has been studied, e.g. in Canale et al. (2010); Ilzhöfer et al. (2007). In Diehl et al. (2005) a real-time iteration scheme is considered, where an MPC problem with nonlinear kite dynamics is solved by iteratively linearising around past solutions. In this work, we consider a path following method, similar to the approach in Liniger et al. (2015), where the dynamics are linearised around the reference path. We design a model predictive guidance controller that minimises the deviation from a reference path while satisfying constraints imposed by the limitations of the lower-level tracking controller that are subject to model uncertainty and input delay.

2. CONTROL SCHEME

We consider a two-line tethered kite system in the traction phase. The wing is flown in crosswind conditions while the tethers are slowly reeled out in order to generate power. The control of the tether length is decoupled from the flight controller which steers the kite to achieve figure-of-eight flight paths. The steering input, δ, is the difference in line length between the right and the left line. The position of the kite in Cartesian coordinates,

$$p = \begin{bmatrix} p_x \\ p_y \\ p_z \end{bmatrix} = \begin{bmatrix} r\cos(\theta)\cos(\phi) \\ r\cos(\theta)\sin(\phi) \\ r\sin(\theta) \end{bmatrix}, \tag{1}$$

is obtained from measurements of the elevation angle, θ, the azimuth angle, ϕ, and line length, r. Note that θ is defined as the angle from the ground plane towards the kite positions, see Figure 1.

For flight control of autonomous kites the heading angle, γ, has proven to be a suitable feedback control variable. It has been defined in Fagiano et al. (2014) as,

$$\gamma = \arctan\left(\frac{\cos(\theta)\dot{\phi}}{\dot{\theta}}\right), \tag{2}$$

and is the angle between the local north of the kite and the projection of the kite velocity onto the tangent plane of the wind window at the kite position. We further consider the control model presented in Wood et al. (2015b),

$$\dot{\gamma}(t) = K\delta(t - t_d), \tag{3a}$$
$$\dot{\theta}(t) = \frac{v_{\theta\phi}}{r}\cos(\gamma(t)), \tag{3b}$$
$$\dot{\phi}(t) = \frac{v_{\theta\phi}}{r\cos(\theta(t))}\sin(\gamma(t)), \tag{3c}$$

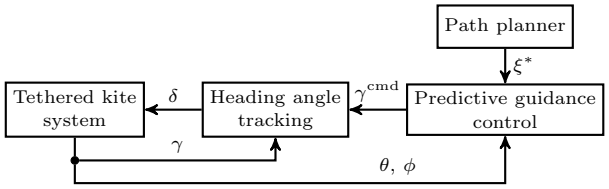

Fig. 2. Cascaded control architecture where the inner loop controls the heading angle, γ, given the signal commanded by the outer loop guidance controller, γ^{cmd}, based on the deviations of the line angles, θ and ϕ, from the reference figure-of-eight path, ξ^*.

where the model parameters consist of the delay, t_d, the tangential velocity of the kite, $v_{\theta\phi}$, the line length, r, and the steering gain, K. We assume that these parameters vary only slowly such that they can be approximated as constants within the control horizon and are adapted online based on updated measurements.

2.1 Cascaded Control

Model (3) is nonlinear and subject to significant input delay, t_d. As shown in Figure 2, we split the problem of following the figure-of-eight path, ξ^*, into two parts: the linear steering model (3a) is used in a low-level controller for tracking a commanded signal, γ^{cmd}; this commanded signal is produced by the predictive guidance strategy based on the nonlinear model given in (3b) and (3c).

Starting from the control approach presented in Wood et al. (2015b), we propose an improved guidance control in this work to ensure the ability of the low-level controller to track the commanded signal. In a path-planning step a periodic reference figure-of-eight path in the (θ, ϕ)-plane is obtained by designing the corresponding flight direction as a sinusoidal function which renders a closed figure-of-eight trajectory according to the model equations (3b) and (3c). The resulting reference path, denoted by $\xi^* = (\theta^*, \phi^*)$, is parametrised by the cycle frequency ω^*.

As the model used in the low-level controller is linear, a frequency domain robustness analysis can be performed to identify and parametrise the limitations of the tracking controller. In contrast to the high-level controller considered in Wood et al. (2015b), the guidance controller presented in Section 3 accounts for constraints that restrict the position of the kite in the wind window and, more crucially, shape the commanded heading angle signal in a way that it can be tracked by the low-level controller.

In Wood et al. (2015a) the low-level tracking controller is designed as a Smith predictor. A nominal proportional controller, C_0, is designed assuming an idealised delay-free plant, $\gamma = G_0(s)\delta$, where we use operator notation to denote the input δ being applied to the linear system with transfer function $G(s)$. The delay is accounted for in the system model,

$$G(s) = G_0(s)e^{-st_d} = \frac{K}{s}e^{-st_d}, \tag{4}$$

used in the design of the controller,

$$C(s) = \frac{C_0}{1 + C_0 G_0(s)(1 - e^{-st_d})}. \tag{5}$$

Neglecting any model mismatch this controller achieves a closed-loop response, $\gamma = T(s)\gamma^{\text{cmd}}$, that is the same as the desired nominal response shifted by the time delay,

$$T(s) = \frac{L(s)}{1+L(s)} = \frac{L_0(s)}{1+L_0(s)} e^{-st_d} = T_0(s)e^{-st_d} \tag{6}$$

with $L_0(s) := C_0 G_0(s)$ and $L(s) := C(s)G(s)$.

2.2 Limitations of the Tracking Controller

To generate signals that can be tracked reliably by the Smith predictor (5) we derive a bound on the rate of the commanded signal such that robust tracking performance is guaranteed when considering uncertainty in the steering gain, K, and time delay, t_d. This bound, l_r, is taken into account as an input rate constraint in the optimisation performed in the guidance presented in Section 3.

We consider a model uncertainty description for first order linear systems with input delay given in Laughlin et al. (1987). That is, we consider the perturbed transfer functions, $G^p(s)$, in the set

$$\mathcal{G} := \left\{ \left(1 + W_m(s)\Delta(s)\right) G(s) \middle| \|\Delta(s)\|_\infty \leq 1 \right\},$$

where the uncertainty weight satisfies,

$$W_m(j\omega) = \begin{cases} \left| \frac{K+\delta K}{K} e^{-j\delta t_d \omega} - 1 \right| & \text{if } \omega < \frac{\pi}{\delta t_d}, \\ \left| \frac{K+\delta K}{K} \right| + 1 & \text{if } \omega \geq \frac{\pi}{\delta t_d}, \end{cases}$$

with δK and δt_d being the largest considered deviations of the model parameters from the estimated values used in the plant model (4). $\Delta(s)$ is the unknown but bounded perturbation.

The Smith predictor in (5) can be interpreted as the application of the nominal control gain, C_0, to the signal $\gamma^{\text{cmd}} - \hat{\gamma}_{t_d}$, where $\hat{\gamma}_{t_d} := \gamma + G_0(s)(1 - e^{-st_d})\delta$ is the prediction of the value of γ, t_d ahead of time, given its current value and the past control inputs.

In the guidance control design we assume that the heading angle follows the commanded value with a time delay, $\gamma(t) \approx \gamma^{\text{cmd}}(t - t_d)$. For evaluating the performance of the tracking controller we therefore consider the closed-loop transfer function, $S_{t_d}(s)$, between the steering input, $\delta(t)$, and the shifted tracking error $e_{t_d}(t) := \gamma^{\text{cmd}}(t) - \gamma(t + t_d)$. Assuming no parameter mismatch we have $S_{t_d}(s) = S_0(s)$; considering perturbed plants $G^p(s) \in \mathcal{G}$ we have,

$$S^p_{t_d}(s) = \frac{1 + L(s)(1 - e^{st_d}) + L(s)(1 - e^{st_d})W_m(s)\Delta(s)}{1 + L(s) + L(s)W_m(s)\Delta(s)}.$$

To keep the shifted tracking error small we bound the magnitude of the commanded signal, $|\gamma^{\text{cmd}}| \leq l_m$, and its derivative, $|\dot{\gamma}^{\text{cmd}}| \leq l_r$. This objective is approximately described in the frequency domain with the performance specification of ensuring $|e_{t_d}(\omega)| < b_e$ while $|\gamma^{\text{cmd}}(\omega)| \leq l_m$, $|\omega\gamma^{\text{cmd}}(\omega)| < l_r$, for all frequencies ω. To capture this specification, we define the performance weight,

$$W_p(j\omega) = \begin{cases} \frac{l_m}{b_e} & \text{if } \omega < \frac{l_r}{l_m}, \\ \frac{l_r}{b_e \omega} & \text{if } \omega \geq \frac{l_r}{l_m}. \end{cases} \tag{7}$$

Satisfying the performance specification robustly is equivalent to

$$\sup_{\|\Delta\|_\infty \leq 1} \|W_p(j\omega) S^p_{t_d}(j\omega)\|_\infty < 1. \tag{8}$$

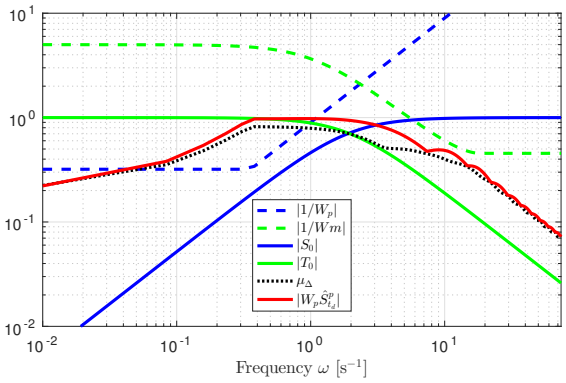

Fig. 3. Robustness analysis for typical parameter values. The red line captures the right-hand of (9); the black dotted line depicts the structured singular value.

Given the control, model, and weighting parameters, C_0, K, t_d, δK, δt_d, l_m, b_e, and l_r, upper and lower bounds for $\sup_{\|\Delta\|_\infty \leq 1} \|W_p(j\omega) S^p_{t_d}(j\omega)\|_\infty$ can be found numerically by structured singular value analysis. To select the parameter l_r from a closed-form expression such that robust performance is guaranteed we consider a sufficient analytic condition for satisfying (8),

$$\begin{aligned} 1 > |W_m(j\omega)T_0(j\omega)| \left(1 + |W_p(j\omega)||1 - e^{j\omega t_d}|\right) \\ + |W_p(j\omega)S_0(j\omega)|, \end{aligned} \tag{9}$$

for all frequencies ω. See Appendix A for this derivation.

Based on (7) and (9), the sufficient condition on robust performance depends on the derivative of the signal that is to be tracked. For larger time delays, the roll-off frequency of the performance weight in (7) has to be lower to ensure robust tracking performance. Assuming a fixed upper bound on the magnitude of the commanded signal, l_m, and given a nominal control gain, C_0, the time delay, t_d, and the uncertainty levels, δK and δt_d, lead to an upper bound on the rate of the commanded signal, l_r, for which robust performance is guaranteed by (9).

An example of the closed-loop transfer function magnitudes, weighting functions, and robustness analysis functions for typical parameter values observed in experiments is shown in Figure 3. The inverse of the weighting functions are plotted to illustrate that nominal performance and robust stability are satisfied because $|S_0|$ lies below $\frac{1}{|W_p|}$ and $|T_0|$ lies below $\frac{1}{|W_m|}$ respectively. Considering 20% uncertainty in the model parameters, $\delta K = 0.2K$, $\delta t_d = 0.2t_d$, robust tracking of the commanded signal with maximal tracking error $b_e = 0.8$, is guaranteed if the red line representing the right hand side of (9), denoted as $|W_p \hat{S}^p_{t_d}|$, remains below 1. The nominal control gain, $C_0 = -0.83$ m, and the bound on the rate of the commanded signal, $l_r = 0.89$ s^{-1}, have been selected such that this is the case. The dotted black line shows the value of the structured singular value that calculates the left hand side of (8) accurately for this case. We observe the gap between the red and the dotted black line to assess the conservativeness of the sufficient condition given in (9).

3. GUIDANCE CONTROL

In the guidance we consider a model-based optimisation approach and assume perfect delay compensated tracking

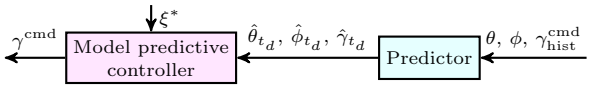

Fig. 4. Guidance control consisting of a prediction of the state after the dead time $(\hat{\gamma}_{t_d}, \hat{\theta}_{t_d}, \hat{\phi}_{t_d})$ and a path-following MPC.

in the low-level controller, $\gamma(t) = \gamma^{\text{cmd}}(t - t_d)$. The objective is to find a commanded heading angle, γ^{cmd}, that minimises the deviation of position trajectory in line angles, $\xi = (\theta, \phi)$, from the reference figure-of-eight path, $\xi^* = (\phi^*, \theta^*)$, while satisfying constraints on the position and the commanded signal. The rate of the commanded signal is bound such that it satisfies the limits of the tracking controller discussed in Sections 2.2, $|\dot{\gamma}^{\text{cmd}}| \leq l_r$. Constraint satisfaction is the main advantage of the method presented here in comparison to the unconstrained approach introduced in Wood et al. (2015b).

3.1 Delay Compensation

The input delay of the steering dynamics carries through to the guidance control. The value of the commanded heading angle at time t does not affect the position until time $t + t_d$. A delay compensating scheme, where the predicted values of the state after the delay time, t_d, are fed to the MPC, is applied as illustrated in Figure 4.

By applying forward Euler discretisation to the model equations (3b) and (3c) we obtain a discrete-time model, $\xi_{k+1} := [\theta_{k+1}\ \phi_{k+1}]^\top = f_d(\xi_k, \gamma_k)$, where k denotes the discrete time step with sampling time, T_s, and d is an integer such that $t_d = dT_s$. This model and the assumption $\gamma_k = \gamma^{\text{cmd}}_{k-d}$ is used to predict the positions d-steps ahead of time, $\hat{\xi}_{k+d}$, given the current positions, ξ_k, and the d past commanded heading angles, $\gamma^{\text{cmd}}_{\text{hist}} := (\gamma^{\text{cmd}}_{k-d}, \gamma^{\text{cmd}}_{k-d+1}, \ldots, \gamma^{\text{cmd}}_{k-1})$.

3.2 Predictive Path Following

The reference figure-of-eight path is generated in the path-planning step discussed in Section 2.1. The path is discretised, $\xi^* = (\xi^*_1, \xi^*_2, \ldots, \xi^*_N)$, $\xi^*_i = (\theta^*_i, \phi^*_i)$, such that it is periodic and fulfils the system dynamics, i.e. there exists a sequence of reference directions, $\gamma^* = (\gamma^*_1, \gamma^*_2, \ldots, \gamma^*_N)$, such that $(\theta^*_{i+1}, \phi^*_{i+1}) = f_d(\theta^*_i, \phi^*_i, \gamma^*_i)$, for $i = 0, 1, \ldots, N-1$ and $(\theta^*_1, \phi^*_1) = f_d(\theta^*_N, \phi^*_N, \gamma^*_N)$.

We linearise the dynamics around the reference trajectory, starting at the closest point from the d-step ahead prediction, ξ_l. and obtain a linear time-varying deviation system, $\chi_{i+1} \approx A_i\chi_i + B_i u_i$, where $\chi_i := \hat{\xi}_{k+d+i} - \xi^*_{l+i}$, $u_i := \gamma^{\text{cmd}}_{k+i} - \gamma^*_{l+i}$, $A_i := \frac{\partial f}{\partial \xi}(\xi^*_{l+i}, \gamma^*_{l+i})$, and $B_i := \frac{\partial f}{\partial \gamma}(\xi^*_{l+i}, \gamma^*_{l+i})$.

The commanded heading angle is determined by the optimiser of the following optimisation problem:

$$
\begin{aligned}
\min_{u,\epsilon} \quad & \sum_{i=0}^{H-1} \left(\chi_i^\top Q \chi_i + R u_i^2 + \epsilon_i^\top S \epsilon_i\right) + \chi_H^\top Q_H \chi_H + \epsilon_H^\top S_H \epsilon_H \,, \\
\text{s.t.} \quad & \chi_i = A_i \chi_i + B_i u_i \,, \qquad (10) \\
& \underline{\chi}_i \leq \chi_i + \epsilon_i \,, \quad \chi_i - \epsilon_i \leq \overline{\chi}_i \,, \quad \epsilon_i \geq 0 \,, \\
& \underline{u}_i \leq u_i \leq \overline{u}_i \,, \quad \underline{\Delta u}_i \leq \Delta u_i \leq \overline{\Delta u}_i \,,
\end{aligned}
$$

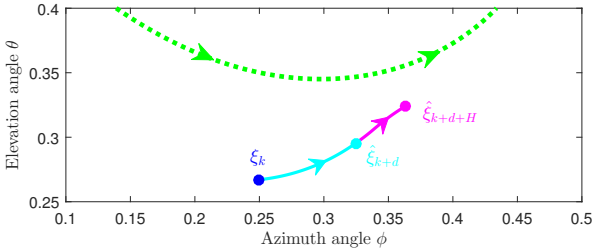

Fig. 5. Predicted position trajectory given the current state (blue), delay compensation of $t_d = 0.54$s (cyan), and MPC prediction of 0.3s (magenta) for following a reference figure-of-eight path (green).

with the input sequence $u := (u_0, u_1, \ldots, u_{H-1})$, slack variable sequence $\epsilon := (\epsilon_1, \epsilon_2, \ldots, \epsilon_H)$, slew rate $\Delta u_i := u_i - u_{i-1}$, and diagonal, positive-definite cost weighting matrices Q, Q_H, R, S, S_H.

The slack variables ensure that the state constraints, with $\underline{\chi} = \xi_{\min} - \xi^*_{l+i}$ and $\overline{\chi} = \xi_{\max} - \xi^*_{l+i}$, are soft. That is, the limits on the kite position, $\xi_{\min}$, $\xi_{\max}$ can be violated with high penalisation, $S \gg Q$, $S_H \gg Q_H$. The soft constraints prevent the optimisation problem from becoming infeasible when there is no possibility of satisfying the bounds on the position. This is important for the application to autonomous kites, particularly, when initialising the controller.

The input bounds, $\underline{u}_i := -l_m - \gamma^*_{l+i}$, $\overline{u}_i := l_m - \gamma^*_{l+i}$, with $l_m < \pi$, limit the magnitude of the commanded heading angle and prevent the guidance controller from commanding the kite to fly straight down towards the ground. The slew rate bounds, $\underline{\Delta u}_i := -l_r T_s - (\gamma^*_{l+i} - \gamma^*_{l+i-1})$, $\overline{\Delta u}_i := l_r T_s - (\gamma^*_{l+i} - \gamma^*_{l+i-1})$, limit the rate at which the commanded flight direction can change. This bound is crucial in this control scheme and is to be set in correspondence with the tracking limitations discussed in Section 2.2 to ensure good control performance.

Note that the kite dynamics are predicted up to $d+H$ steps ahead of the current time step. The first d time steps of the prediction are given by the d past inputs and the nonlinear system model. The second part of the prediction with length H depends on the current and future inputs based on the linearised time-varying system model. Figure 5 illustrates the combined prediction horizon of the predictor and MPC block.

The commanded heading angle is set to be the first element of the optimal sequence, u^{opt}, that solves (10), $\gamma^{\text{cmd}}_k = u^{\text{opt}}_0 + \gamma^*_l$. The optimisation is repeated in every discrete time step with a receding horizon.

4. RESULTS

The control scheme is implemented in MATLAB SIMULINK running on a Speedgoat real-time target machine and tested with the high fidelity kite simulation framework presented in Gohl and Luchsinger (2013). This kite simulation tool contains a quasi-steady three-dimensional model of the kite aerodynamics and a tether model that accounts for line dynamics and line stretching. The real-time target machine running the controller is the same hardware as used in real-world experiments in the Autonomous Airborne Wind Energy (A2WE) research project. The control

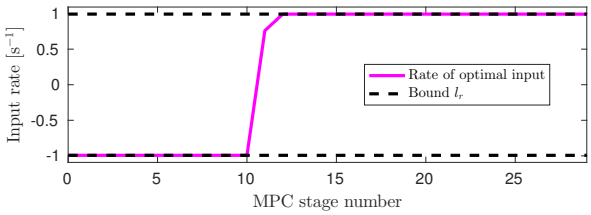

Fig. 6. Rate of change of the optimal input sequence produced by the MPC for the initial condition illustrated in Figure 5 limited by the bound l_r to ensure robust tracking performance of the low-level controller.

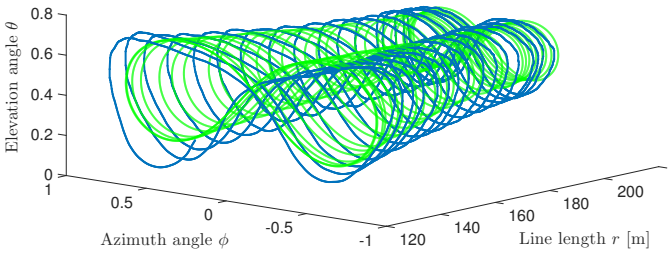

Fig. 7. Trajectory of the kite position (blue) following a varying reference figure-of-eight path, ξ^*, (green) for a simulation with slow line reel-out.

block has access to the simulated measurement variables produced by the simulation tool running on a separate computer via serial connection. The SIMULINK block performs the state estimation, data processing, and control input computation within $T_s = 10$ ms as required in the real-world experiments.

The optimisation problem (10) is solved online. A customised solver is implemented with the optimisation software generation tool FORCES Pro by Domahidi and Jerez (2014). A Primal-Dual Interior-Point method is applied. The input rate constraint is implemented by augmenting the state with the previous input and solving a standard MPC problem with modified dynamics such that the input rate is part of the decision variables. The optimisation horizon is selected to be $H = 30$.

We consider a constant wind speed of 10 ms^{-1} aligned in the direction of the x-axis. The winch control is simulated to follow a function linking the line force and the reel-out speed. Measurement noise is simulated and a state estimation approach as in Fagiano et al. (2014) is applied to obtain position and velocity estimates. The model parameters in (3) are estimated online and adapted throughout the simulation to changing conditions as suggested in Wood et al. (2015a). Despite not including wind variation in the simulation the estimated model parameters vary depending on the flight conditions as a result of varying line lengths, flight patterns and winch settings.

We set the weights in the MPC cost function to be $Q = \text{diag}(1, 2)$, $Q_H = 5 \cdot Q$, $R = 5 \cdot 10^{-3}$, $S = 10^5 \cdot Q$, and $S_H = 10^5 \cdot Q_H$. The bound on the magnitude of the commanded signal is $l_m = 2.5$. Considering 20% uncertainty in t_d and K, the control gain, C_0, is set adaptively to the maximal value such that robust stability is satisfied and the bound on the rate of the commanded signal, l_r, is subsequently set to the maximum value such that the robust performance condition (9) is satisfied.

Figure 5 shows the flight path predicted by the guidance controller. Given the estimated position of the kite in terms of line angles, (θ, ϕ), shown in blue, the predicted position of the kite after the delay time is computed in the predictor block and illustrated in cyan. The MPC minimises the further evolution of the kite with an input rate constraint of $l_r = 0.99$ s^{-1} which satisfies Equation (9). The predicted path applying the optimal input sequence, u^{opt}, is shown in magenta. The corresponding derivative of the optimiser sequence is plotted in Figure 6. In this example, the rate hits the rate constraints. That is, in this situation the commanded turn rate is limited in order to respect the bound imposed by the underlying velocity vector orientation tracking controller.

Next, we consider a simulation with slow line reel out from 124m to 216m in 300s. The reel-out speed is a function of the line forces resulting in a non-uniformly increasing line length. Figure 7 shows the trajectory of the line angles throughout the simulation in blue. The trajectory follows varying figure-of-eight paths shown in green. Note that despite the figure-of-eight cycles appearing smaller in the (θ, ϕ)-plane for longer line lengths, the actual path length per cycle in (x, y, z)-coordinates is increasing.

As the line length, the velocity and actuation pattern change, the forces acting on the wing and the lines vary. These variations influence the dynamics. To account for the changing operating conditions the model, parameters are re-estimated twice per figure-of-eight cycle. With varying model parameters the reference path, ξ^*, and the control parameters are also changed. In particular, the rate limit, l_r, is adapted to the increasing delay observed with increasing tether length. Figure 8 shows the evolution of the model parameters and the adapted rate limit to ensure good tracking performance throughout.

5. CONCLUSION

An optimisation based MPC path-following guidance has been designed that accounts for limitations of the underlying tracking controller in a cascaded control architecture for a kite system affected by input delay. The limitations of the tracking controller arise from uncertainty in the model used for delay compensation and feedback control. Good tracking performance can be guaranteed despite these limitations by limiting the rate of the commanded signal produced by the guidance controller. This is encoded into the optimisation problem as input rate constraint.

Given delay compensated predictions, the MPC is based on dynamics that are linearised around the reference path. The models applied are of low order and neglect variations of slowly evolving variables such as the line length or the input delay. Instead, these parameters are updated online based on current measurement data. Consequently, the bounds on the limitations are adapted to account for the varying operating conditions.

The path-following control method has been successfully tested in a hardware-in-the-loop simulation study on a real-time computer running at a sampling time of 10 ms. Future work will include disturbance models in the analysis of the control limitations.

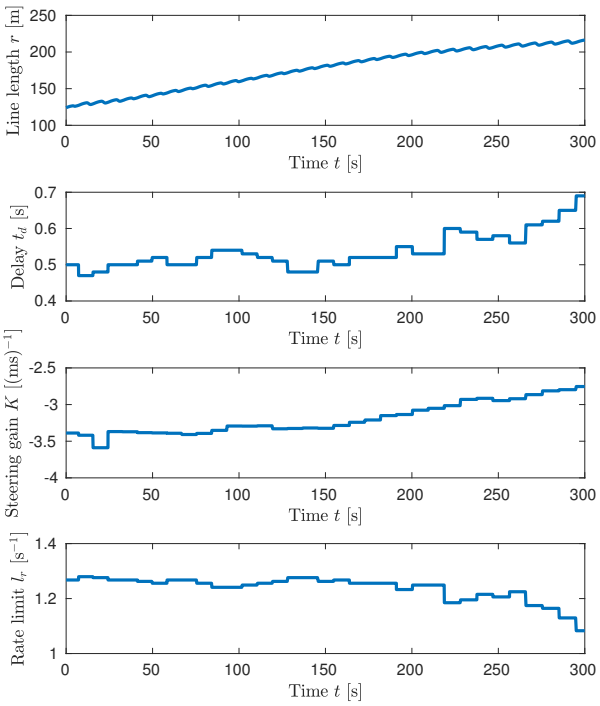

Fig. 8. Evolution of the estimated model parameters and the rate limit of commanded heading angle, l_r, for the simulation study shown in Figure 7.

REFERENCES

Ahrens, U., Diehl, M., and Schmehl, R. (2013). *Airborne wind energy*. Springer.

Canale, M., Fagiano, L., and Milanese, M. (2010). High Altitude Wind Energy Generation Using Controlled Power Kites. *IEEE Transactions on Control Systems Technology*, 18(2), 279–293.

Diehl, M., Bock, H.G., and Schlöder, J.P. (2005). A Real-Time Iteration Scheme for Nonlinear Optimization in Optimal Feedback Control. *SIAM Journal on control and optimization*, 43(5), 1714–1736.

Domahidi, A. and Jerez, J. (2014). FORCES Professional. embotech GmbH (`http://embotech.com/FORCES-Pro`).

Erhard, M. and Strauch, H. (2013a). Control of Towing Kites for Seagoing Vessels. *IEEE Transactions on Control Systems Technology*, 21(5), 1629–1640.

Erhard, M. and Strauch, H. (2013b). Theory and Experimental Validation of a Simple Comprehensible Model of Tethered Kite Dynamics used for Controller Design. In *Airborne wind energy*, 141–165. Springer.

Fagiano, L., Zgraggen, A.U., Morari, M., and Khammash, M. (2014). Automatic Crosswind Flight of Tethered Wings for Airborne Wind Energy: Modeling, Control Design, and Experimental Results. *IEEE Transactions on Control Systems Technology*, 22(4), 1433–1447.

Gohl, F. and Luchsinger, R.H. (2013). Simulation Based Wing Design for Kite Power. In *Airborne Wind Energy*, 325–338. Springer.

Ilzhöfer, A., Houska, B., and Diehl, M. (2007). Nonlinear MPC of Kites under Varying Wind Conditions for a New Class of Large-Scale Wind Power Generators. *Int. Journal of Robust and Nonlinear Control*, 17(17), 1590–1599.

Laughlin, D.L., Rivera, D.E., and Morari, M. (1987). Smith Predictor Design for Robust Performance. *Int. Journal of Control*, 46(2), 477–504.

Liniger, A., Domahidi, A., and Morari, M. (2015). Optimization-Based Autonomous Racing of 1: 43 Scale RC Cars. *Optimal Control Applications and Methods*, 36(5), 628–647.

Polzin, M., Wood, T.A., Hesse, H., and Smith, R.S. (2017). State Estimation for Kite Power Systems with Delayed Sensor Measurements. In *IFAC World Congress*. Toulouse, France.

Rontsis, N., Costello, S., Lymperopoulos, I., and Jones, C.N. (2015). Improved Path Following for Kites with Input Delay Compensation. In *Conf. on Decision and Control*, 656–663. Osaka, Japan.

Wood, T.A., Hesse, H., Zgraggen, A.U., and Smith, R.S. (2015a). Model-Based Identification and Control of the Velocity Vector Orientation for Autonomous Kites. In *American Control Conf.*, 2377–2382. Chicago, IL, USA.

Wood, T.A., Hesse, H., Zgraggen, A.U., and Smith, R.S. (2015b). Model-Based Flight Path Planning and Tracking for Tethered Wings. In *Conf. on Decision and Control*, 6712–6717. Osaka, Japan.

Zgraggen, A.U., Fagiano, L., and Morari, M. (2015). Automatic Retraction and Full-Cycle Operation for a Class of Airborne Wind Energy Generators. *IEEE Transactions on Control System Technology*, 24(2), 594–608.

Appendix A. ROBUST PERFORMANCE

In this section we derive the sufficient condition given in (9) for robust performance defined in (8). We start by finding an upper bound on $\sup_{|\Delta(j\omega)|\leq 1} |S^p_{t_d}(j\omega)|$,

$$
\begin{aligned}
&\sup_{|\Delta(j\omega)|\leq 1} |S^p_{t_d}(j\omega)| \\
\leq &\frac{\sup_{|\Delta(j\omega)|\leq 1} |1 + L(j\omega)(1 - e^{j\omega t_d})(1 + W_m(j\omega)\Delta(j\omega))|}{\inf_{|\Delta(j\omega)|\leq 1} |1 + L(j\omega)(1 + W_m(j\omega)\Delta(j\omega))|} \\
= &\frac{|1 + L(j\omega)(1 - e^{j\omega t_d})| + |L(j\omega)(1 - e^{j\omega t_d})W_m(j\omega)|}{|1 + L(j\omega)| - |L(j\omega)W_m(j\omega)|}
\end{aligned}
$$

By applying $S_0(j\omega) + T_0(j\omega) = 1$, $S(j\omega) + T(j\omega) = 1$, and (6), we get a sufficient condition for robust performance if the following holds for all frequencies ω,

$$
\begin{aligned}
1 > &|W_m(j\omega)| \frac{|L(j\omega)|}{|1 + L(j\omega)|} \\
&+ |W_m(j\omega)W_p(j\omega)| \frac{|L(j\omega)(1 - e^{j\omega t_d})|}{|1 + L(j\omega)|} \\
&+ |W_p(j\omega)| \frac{|1 + L(j\omega)(1 - e^{j\omega t_d})|}{|1 + L(j\omega)|} \\
= &|W_m(j\omega)T(j\omega)| \\
&+ |W_m(j\omega)W_p(j\omega)T(j\omega)(1 - e^{j\omega t_d})| \\
&+ |W_p(j\omega)||S(j\omega) + T(j\omega) - T_0(j\omega)| \\
= &|W_m(j\omega)T_0(j\omega)| \\
&+ |W_m(j\omega)T_0(j\omega)||W_p(j\omega)(1 - e^{j\omega t_d})| \\
&+ |W_p(j\omega)||1 - T_0(j\omega)| \\
= &\, |W_m(j\omega)T_0(j\omega)| \left(1 + |W_p(j\omega)||1 - e^{j\omega t_d}|\right) \\
&+ |W_p(j\omega)S_0(j\omega)| \,.
\end{aligned}
$$